JOURNAL OF BACTERIOLOGY, Dec. 2010, p. 6217–6229 Vol. 192, No. 23
0021-9193/10/$12.00 doi:10.1128/JB.00106-10

HU Protein Affects Transcription of Surface Polysaccharide Synthesis Genes in *Porphyromonas gingivalis*▽†

Christine Alberti-Segui,[1]‡ Annette Arndt,[1]§ Carla Cugini,[1] Richa Priyadarshini,[1] and Mary E. Davey[1,2]*

Department of Molecular Genetics, The Forsyth Institute, Boston, Massachusetts,[1] and Department of Oral Medicine Infection and Immunity, Harvard School of Dental Medicine, Boston, Massachusetts[2]

Received 29 January 2010/Accepted 15 September 2010

K-antigen capsule synthesis is an important virulence determinant of the oral anaerobe *Porphyromonas gingivalis*. We previously reported that the locus required for synthesis of this surface polysaccharide in strain W83 (TIGR identification PG0106 to PG0120) is transcribed as a large (~16.7-kb) polycistronic message. Through sequence analysis, we have now identified a 77-bp inverted repeat located upstream (206 bp) of the start codon of PG0106 that is capable of forming a large hairpin structure. Further sequence analysis just upstream and downstream of the capsule synthesis genes revealed the presence of two genes oriented in the same direction as the operon that are predicted to encode DNA binding proteins: PG0104, which is highly similar (57%) to DNA topoisomerase III, and PG0121, which has high similarity (72%) to DNA binding protein HU (β-subunit). In this report, we show that these two genes, as well as the 77-bp inverted repeat region, are cotranscribed with the capsule synthesis genes, resulting in a large transcript that is ~19.4 kb (based on annotation). We also show that a PG0121 recombinant protein is a nonspecific DNA binding protein with strong affinity to the hairpin structure, *in vitro*, and that transcript levels of the capsule synthesis genes are downregulated in a PG0121 deletion mutant. Furthermore, we show that this decrease in transcript levels corresponds to a decrease in the amount of polysaccharide produced. Interestingly, expression analysis of another polysaccharide synthesis locus (PG1136 to PG1143) encoding genes involved in synthesis of a surface-associated phosphorylated branched mannan (APS) indicated that this locus is also downregulated in the PG0121 mutant. Altogether our data indicate that HU protein modulates expression of surface polysaccharides in *P. gingivalis* strain W83.

Prokaryotes, like all cells, sense their environment at their surface, and changes in the cell envelope reflect adjustment strategies. The cell surface is altered for many functions, such as nutrient uptake, secretion, exclusion of toxic compounds, transfer of genetic information, and adherence. It is clear that changes in the presentation of surface structures play an important role in the life cycle (attachment, growth, and dispersal) of bacteria. The presentation of certain structures, such as pili or fimbriae, can enhance attachment, while other structures, such as the capsule, may create a protective barrier and facilitate dissemination. The focus of this study was to begin to determine the molecular mechanisms controlling K-antigen capsule expression in the Gram-negative oral anaerobe *Porphyromonas gingivalis*.

P. gingivalis is a human opportunistic pathogen that persists in the subgingival crevice of the oral cavity. Its proliferation within the subgingival biofilm community is linked to adult periodontitis, a chronic inflammatory disease characterized by destruction of the tissue supporting the teeth, and ultimately, tooth loss (11, 20, 25, 33, 36). Determinants considered important in the virulence of this pathogen include major surface structures, such as membrane vesicles, fimbriae, cysteine proteases, lipopolysaccharide (LPS), and K-antigen capsule (7, 26, 32, 42). Many bacteria synthesize a dense matrix of capsular polysaccharide on the cell surface, and these surface structures (capsules) greatly influence the cell's interaction with its surroundings. Capsules can provide protection against desiccation, osmotic stress, oxygen toxicity, and phagocytic engulfment (14, 47, 56). They also play an important role in modulating cell-to-cell aggregation and biofilm development in *Escherichia coli* (28, 49), *Vibrio vulnificus* (27), *Neisseria meningitidis* (16), and *P. gingivalis* (15). The K-antigen capsule of *P. gingivalis* is considered a key virulence factor (52). Encapsulated strains disseminate, causing a spreading type of infection in mice, with recovery from blood, spleen, and kidneys after subcutaneous inoculation, while K-antigen null strains typically result in localized abscesses and are significantly less virulent in soft tissue destruction (17, 31). Also, it was recently reported that mice immunized with purified K-antigen capsule were protected against oral bone loss when challenged with *P. gingivalis* (24). With regards to interaction with the human host, the presence and type of capsule has been found to influence the initial adhesion of *P. gingivalis* to human periodontal pocket epithelial cells (17) and to reduce the immune response of human gingival fibroblasts (7). Furthermore, the majority of clinical *P. gingivalis* strains isolated from patients with destructive periodontal disease synthesize K-antigen capsule (30), indicating a link between the disease state and the proliferation of an encapsulated phenotype.

* Corresponding author. Mailing address: Department of Molecular Genetics, The Forsyth Institute, 140 The Fenway, Boston, MA 02115. Phone: (617) 892-8513. Fax: (617) 892-8432. E-mail: mdavey@forsyth.org.

† Supplemental material for this article may be found at http://jb.asm.org/.

‡ Present address: BioMérieux, Biomarker Research Department, Grenoble, France.

§ Present address: Institute of Microbiology and Biotechnology, University of Ulm, Ulm, Germany.

▽ Published ahead of print on 1 October 2010.

HU is a small, basic, heat-stable DNA binding protein that is capable of wrapping DNA and preventing denaturation under detrimental conditions (19, 41, 51). It is a major component of the bacterial nucleoid and shares with eukaryotic histones the ability to introduce negative supercoiling into relaxed DNA in the presence of topoisomerase I, *in vitro* (4). HU is conserved in either its heterodimeric form (HUαβ) or in one of its homodimeric forms ($HU\alpha_2$ or $HU\beta_2$) in virtually every bacterial species. Annotation of the *P. gingivalis* genome indicates that this bacterium has both the β- (PG0121) and the α- (PG1258) subunits. Studies examining HU's function have been primarily performed in *E. coli* and *Bacillus subtilis*. Functions attributed to HUs typically involve changes in DNA architecture (51) and include the ability to stimulate transcription (37) and translation (2). HU binds with low affinity and without sequence specificity to both double-stranded DNA and double-stranded RNA, but it recognizes with high affinity cruciform DNA structures or DNA molecules with a nick or a gap (5, 44, 45). Furthermore, it has been shown that HU binds specifically to nicked or gapped DNA-RNA hybrids and to small noncoding RNA molecules (3).

Loss of HU function results in lethality in *B. subtilis*, a result shared with all other Gram-positive organisms tested to date (21, 29, 51). However, *E. coli* cells that are defective in HU function are viable, but the mutant strains do present a variety of growth defects. *E. coli* cells deficient in expression of both the α- and β-subunits demonstrate increased sensitivity to UV and ionizing radiation (6, 34, 35), have a lethal phenotype following cold or heat shock (23, 53), are defective in cell division (18), and are altered in outer membrane protein composition (43). Recently, the HU regulon was identified in *E. coli* based on transcription profiling of strains deficient in one or both HU subunits (41). This study discovered that HU regulates the expression of 8% of the genome, specifically, genes involved in the response to anaerobiosis, acid stress, high osmolarity, and SOS induction.

Despite the importance of capsular polysaccharide to the virulence and life cycle of *P. gingivalis*, little is known as to how expression of K-antigen capsule synthesis is regulated in this oral anaerobe. Here, we show that the K-antigen capsule synthesis genes are downregulated and capsular polysaccharide production is deficient in a PG0121 (HUβ) mutant strain. This is the first report on HU protein function in *P. gingivalis*.

MATERIALS AND METHODS

Strains, media, and chemicals. Bacterial strains and plasmids used in this study are shown in Table 1. *P. gingivalis* strains were maintained in a COY anaerobic chamber on Trypticase soy agar plates supplemented with 5% defibrinated sheep blood, hemin, and menadione (BAPHK; North-East Laboratory, Waterville, ME). For liquid culture the strains were grown in Trypticase soy broth (TSBHK) or Todd-Hewitt broth (THBHK), also supplemented with hemin and menadione. All media used to grow *P. gingivalis* contained hemin (1 μg/ml) and menadione (1 μg/ml). *E. coli* strains were grown aerobically on Luria-Bertani (LB) plates. Antibiotics were added at the following concentrations: for *E. coli*, ampicillin (Amp) at 100 μg/ml and erythromycin (Erm) 200 μg/ml; for *P. gingivalis*, erythromycin (Erm) at 5 μg/ml and tetracycline (Tc) at 0.5 μg/ml. Unless otherwise stated, all chemicals were obtained from Sigma. Plasmids were constructed in *E. coli* DH5α or BL21(DE3) and then transformed into *P. gingivalis* by electroporation or conjugation (see the protocols below).

Sequence analysis. The Bioinformatics Resource for Oral Pathogens (BROP) at the Forsyth Institute (http://www.brop.org/) (9) was used to obtain the *P. gingivalis* strain W83 sequence and to analyze predicted open reading frames (ORFs). Information from two independently annotated databases, The Comprehensive Microbial Resource of The Institute of Genomic Research (TIGR CMR) and the Oral Pathogen Sequence Databases of Los Alamos National Laboratory (LANL), is currently available on the BROP website. BROP Genome Viewer is a tool that presents information annotated by four different sources (TIGR CMR, LANL ORALGEN, the National Center for Biotechnology Information [NCBI] GenBank record, and BROP). BROP Genome Viewer was used to obtain detailed analysis of the genes in the locus, and another interface (Genome Explorer) was used to link to BLAST, InterProScan, and SwissProt search results. In addition, the program einverted, which was provided by EMBOSS (46), is also available at BROP and was used to identify and search for inverted repeats. Mfold, at http://frontend.bioinfo.rpi.edu/applications/mfold/cgi-bin/dna-form1.cgi, was used for nucleic acid secondary structure analysis (57).

TABLE 1. Strains and plasmids used in this study

Strain or plasmid (relevant genotype or phenotype)	Source or reference
P. gingivalis strains	
W83 (wild type)	C. Mouton, Laval University, Quebec City, Canada
381 (wild type)	H. Kuramitsu, State University of Buffalo, Buffalo, NY
ΔPG0106::Erm (Em^r) in strain W83	Davey and Duncan (15)
ΔPG0121::Erm (Em^r) in strain W83	This study
ΔPG0121::Erm pTgroES HU (Em^r Tc^r) in strain W83	This study
Plasmids	
pHS17	Fletcher et al. (22)
pT-COW (Cb^r Tc^r)	Gardner et al. (22a)
pCR-II Topo (Amp^r)	Invitrogen
pET22b(+)	Novagen
pGEM-T-easy	Promega
pT-C121 (Cb^r Tc^r)	This study
pGEM-HU	This study
pTgroES-HU (Cb^r Tc^r)	This study
pTgroES (Cb^r Tc^r)	This study
pTstloop	This study

Generation of cassettes for allelic exchange. To investigate the effect of PG0121 (72% similarity to HUβ subunit) on capsule expression, we created a deletion mutant. The cassette for allelic exchange to create this knockout strain was generated by overlap PCR, as previously described (15). In brief, three individual DNA amplicons were amplified with primers designed to overlap with one another. All primers are presented in Table 2. The PCR was carried out in 100-μl volumes using the Platinum High-Fidelity SuperMix reaction mixture (Invitrogen). The PCR products were purified by the QIAquick PCR purification protocol (Qiagen). Chromosomal DNA was isolated from *P. gingivalis* W83 with the MasterPure DNA purification kit (Epicentre Biotechnologies, Madison, WI). The coding region for erythromycin resistance (ErmF-ErmAM) was amplified using plasmid pHS17 as a template and primers ErmF and ErmR (22). The PCR to amplify the erythromycin cassette consisted of 30 cycles with a temperature profile of 1 min at 94°C, 30 s at 55°C, and 3 min at 72°C for extension. For amplification of the F3-R2 (~1 kb upstream of PG0121) or the R3-F2 (~1 kb downstream of PG0121) amplicons, the annealing temperature was dropped to 45°C instead of 55°C, since the R2 and F2 primers have nonhybridizing tag sequence on the 5′ end of the primers. To generate the final three-way product, the PCR consisted of 35 cycles with a temperature profile of 1 min at 94°C, 30 s at 40°C, and 6 min at 72°C for extension. The sequence of the final PCR product was confirmed using the F3_121 and R3_121 primers. The PCR product was purified and then transformed as a linear fragment into *P. gingivalis* strain W83 to create the DEL0121::Erm insertion-deletion mutant.

The same protocol was used to generate knockout cassettes for both PG1258 (predicted HUα subunit) and PG0104 (predicted topoisomerase) using primer sets F3/F2_1258 and R3/R2_1258 and F3/F2_0104 and R3/R2_0104, respectively. All primers are presented in Table 2.

Isolation of total RNA. Total RNA was isolated from cells in either the early exponential phase of growth (optical density at 600 nm [OD_{600}] of 0.3), mid-

TABLE 2. Primers used in this study

Primer or probe purpose and name	Sequence (5′–3′)
PG0121 mutant construction, verification, and complementation	
ErmF	CCGATAGCTTCCGCTATTGC
ErmR	GAAGCTGTCAGTAGTATACC
Ermchk1	CGTAAATGTTCAACCAAAGCTGTG
Ermchk2	CTCAAGTCTCGATTCAGCAATTGC
R2_121	TGTAGATAAATTATTAGGTATACTACTGACAGCTTCCTTTTCACGA TTAGTTAGTTAGAC
F2_121	ACCGATGAGCAAAAAAGCAATAGCGGAAGCGATCGGTTCGCGCT ATTTCTTAATTATACA
F3_121	CGAAGCGGTGAAAGCAGGAAC
R3_121	GAAATAGCCGGAAGGGGATAAAGA
FC_121	CGAAGATTGTAGTATAGAATAGAA
RC_121	GTATAATTAAGAAATAGCGCGAAT
BamHI_HU	GGATCCCGATGAACAAGACAGATTTTATTGC
SmaI_HU	CCGGGCGTTACTTAAGTTCCAAAGTAGAGCC
FgroES_Pr	CGCGGATCCGCGATTGGATAGATGCCCTGCTC
RgroES_Pr	CGCGGATCCGCGTGTTGCTTGGTTTGTTATTGTTAG
PG1258 mutant construction	
F3_1258	GGCGGTGGCCATTAAACTTATGT
R3_1258	AGTTGTCCCTCAAGAGTCCCAGAG
F2_1258	ACCGATGAGCAAAAAAGCAATAGCGGAAGCGATCGGTCATAGTT TAACAATAAAACATTA
R2_1258	TGTAGATAAATTATTAGGTATACTACTGACAGCTTCAATACTATG CTCAGAATTAAATGG
PG0104 mutant construction	
F3_0104	TGCGTCACAGTGGGAGAGTAGGA
R3_0104	GCCGACACAAAAACGCTGAAAT
F2_0104	ACCGATGAGCAAAAAAGCAATAGCGGAAGCGATCGGTACTCCCT GCTTTAAGAATCCGGAA
R2_0104	TGTAGATAAATTATTAGGTATACTACTGACAGCTTCGGGCTTATC CTTGATTCTTAAAAA
Northern blot analysis (TIGR primers)	
F0106	AGAACGGTACATAAAGGGGCTATA
R0106	GCTTTGAACTTTTGCCGATAAGAT
F0104	AAGCGGATATGGTCGTGAAC
R0104	CCCCGTGGTTTTGAACTCTA
F0121	TGAATGCCGGAGAGAAAATC
R0121	CGGTTTGAAACGAACAACCT
RT-PCR of K-antigen capsule operon and hairpin region	
RT104	Forward, TAAAGGCTATATGGAGGGCAACG
	Reverse, GCTATCGATGAGTTTGATGCCAA
RT106	Forward, CTTGGTCGGACTATCTTATCGGC
	Reverse, GGCAACTCTTCTATGAATAACAAACCA
TIGR106	Forward, TCTTACATTGCTTTGCGTCG
	Reverse, AAGCAGTATTTGCAATGGGG
RT108	Forward, CATGTGTAGAGGCTGCAAC
	Reverse, GACGCTCTCGATAGATTAGATCAG
RT110	Forward, CTATCGGAGTCGTTCTAAGCCTTG
	Reverse, CAAAATACGGTGCAACCAATACAC
RT113	Forward, CGTCCAGGAGATAGACTGATTGTTAC
	Reverse, TGGTGGATAATAAGGCATCATAATA
RT116	Forward, GGAACAGGTCAAGAAGCTCGC
	Reverse, CGTAGCGCAGAAATTCGTAGC
RT118	Forward, GCGATGAATTGACAGAACAGCAT
	Reverse, TTGCGTAATTTGGCTCATAATAACTG
RT119_F	AGCGATACAGCCGAGAGAAA
RT120_R	CGGAATCTGTTGATAGAAAGCAGC
RT121	Forward, CAGAACAGATGAATGCCGGAGA
	Reverse, GCACGCTCGCTCACTGAGAA
RT_hairpin	Forward, GACATGACCGTCAACAGCAC
	Reverse, TTGGCTGCTACTGTGTACCG

Continued on following page

TABLE 2—*Continued*

Primer or probe purpose and name	Sequence (5′–3′)
RT_end104	Forward, GAAGCTTTCGGTTGCAATG
	Reverse, AATCAATTTTCATCGGACACG
RT_link104	Forward, AATGATGGCTTTGAGTGGATG
	Reverse, GAATCGGGCACCTGTGAG
RT_start106	Forward, CATCGTTGAAAGGATTTGATTG
	Reverse, ATCATCTCTTCTGCCCATCC
RT_link106	Forward, CACTGGGATTTAGGAATATAGACG
	Reverse, AAAATTTCCCCAATGACAAAAC
RT-PCR of A-LPS synthesis locus	
PG1137	Forward, GTGTACTCACGATCGTTGCCAC
	Reverse, ACTGCAGGAATGAGAGCTAAACAG
PG1138	Forward, CGATGATATACTACCCGATACCACTC
	Reverse, CTCTATCTCCATTTCCGGATAGATG
PG1140	Forward, TCGGATCAGCTCACAATATCGG
	Reverse, TGTCGGCACCACTTC
16S	Forward, TGTTACAATGGGAGGGACAAAGGG
	Reverse, TTACTAGCGAATCCAGCTTCACGG
Synthesis of mobility shift assay probes	
F_106Lp	GCACTGGCAATGTAACCT
R_106Lp	AATCATCTCTTCTGCCCATCC
F_106pr	ATTACCTTTGCGCTCTATTA
R_106pr	AATCATCTCTTCTGCCCATCC

exponential phase (OD_{600} of 0.6), or stationary phase (OD_{600} of 1.2). RNA was isolated and purified using the MasterPure RNA purification kit (Epicentre), following the manufacturers' protocol. Purity and integrity of the RNA were assessed as previously described (15).

Northern blotting and reverse transcription-PCR (RT-PCR) analysis. For Northern blot analyses, total RNA was mixed with NorthernMax formaldehyde loading dye (Ambion), heat denatured, and run on a 1% denaturing agarose gel. The amount of RNA loaded in each lane was 12.5 μg. After electrophoresis, the gel was stained with ethidium bromide to confirm that the lanes were equally loaded and to verify that the RNA was not degraded. After electrophoresis the RNA was transferred to a positively charged nylon membrane (Hybond N^+; Amersham) and then cross-linked with a UV Stratalinker (Stratagene). Overnight transfer with 10× SSC (1× SSC is 0.15 M NaCl plus 0.015 M sodium citrate) was used to optimize transfer of large transcripts from the gel to the blot. After transfer, the RNA agarose gel was again stained with ethidium bromide, to confirm transfer of RNA. The probe for detection of PG0106 transcript was a 233-bp PCR amplicon generated from W83 DNA using the F106 and R106 primer set. The probe for the detection of the PG0104 transcript was a 962-bp fragment amplified from W83 DNA using the TIGR_F104 and TIGR_R104 primer set. The probe for detection of PG0121 transcript was a 137-bp fragment amplified from W83 DNA using the TIGR_F121 and TIGR_R121 primer set. All primers are listed in Table 2. It should be noted that the primers with the designation TIGR are primers designed at TIGR to generate the *P. gingivalis* microarray amplicons. These probes are designed for specificity of the target gene. The labeling of the probe, hybridization of the blot, and detection of the signal were performed using the AlkPhos direct labeling and detection kit (GE Healthcare Life Sciences) according to the manufacturer's instructions.

For RT-PCRs, 1 μg of purified total RNA was reverse transcribed with the MonsterScript reverse transcriptase kit, according to the manufacturer's protocol (Epicentre) using random primers. This reverse transcriptase lacks RNase H, enabling improved synthesis of full-length cDNA even for long mRNA. In addition, MonsterScript is thermostable, permitting reverse transcription at 65°C, which reduces RNA secondary structure and improves priming specificity. For synthesis of shorter cDNA fragments, the QuantiTect reverse transcription kit (Qiagen), which provides integrated genomic DNA removal, was used. Gene-specific primers for PCRs are listed in Table 2. The PCR consisted of 35 cycles with a temperature profile of 30 s at 94°C, 30 s at 55°C, and 1 min at 72°C for extension.

qPCR. For cDNA generation, 1 μg of total RNA was reverse transcribed with either a gene-specific primer or random 9-mer primer using the MonsterScript reverse transcriptase kit according to the manufacturer's protocol (Epicentre). Primers were designed by using the free NetPrimer software of PREMIER Biosoft International. The expected product sizes were in the 100- to 200-bp range, and 16S rRNA was used as a reference gene. Quantitative RT-PCR (qPCR) was carried out with a Bio-Rad iCycler using SYBR green supermix (Bio-Rad). The qPCR consisted of an initial denaturation step at 95°C for 3 min followed by 50 cycles with a temperature profile of 15 s at 95°C, 15 s at 60°C, and 15 s at 72°C. A melting curve profile of each amplified PCR product was determined using the following conditions: 1 min at 95°C and 1 min at 55°C, followed by 80 cycles of 10 s each and a temperature increase of 0.5°C per cycle starting at 55°C.

For analysis, we first confirmed that the threshold cycle (C_T) values for all genes were consistent and reproducible in the parent strain; if these C_T values had varied greatly then the analysis could not have been performed. Once this was established, the data were then normalized to 16S, the values from W83 were set to 1, and then the copy number ratios of ΔPG0121, ΔPG0121-pTgroES-HU, and ΔPG0121-pTgroES to the parent strain W83 were determined. This experiment was repeated three times.

Electroporation and conjugation of *P. gingivalis*. Electroporation of cells was performed as previously described (15, 39) with some slight modifications. To prepare competent cells, 2 ml of an actively growing culture of *P. gingivalis* was used to inoculate 200 ml of prewarmed and prereduced TSBHK. The culture was then incubated overnight at 37°C to an OD_{550} of between 0.3 and 0.6. The cells were harvested by centrifugation at 2,600 × *g* for 10 min at 4°C and then washed twice with 200 ml followed by 100 ml of electroporation buffer (EP; 10% glycerol, 1 mM $MgCl_2$; filter sterilized; stored at 4°C). After washing, the pellet was suspended in 1 ml of EP (final volume), aliquoted into microcentrifuge tubes (100 μl/tube), and frozen at −80°C for future use. A 100-μl sample of cells to which 5 μg of DNA (linear DNA fragments) was added was placed in a sterile electroporation cuvette (0.2-cm gap). The cells were pulsed with a Bio-Rad gene pulser at 2,500 V, and then 1 ml of TSBHK was added and the mixture was incubated anaerobically at 37°C for 18 h. The cells were concentrated by centrifugation, and the entire sample was plated on BAPHK containing erythromycin (5 μg/ml) for selection of deletion mutants.

Conjugation was used to transfer large plasmids (pT-COW and its derivatives) from *E. coli* (strain S17-1, which contains the transfer functions of R4 integrated into the chromosome) into *P. gingivalis*. The method used was as previously described (10). However, for selection we did not incubate the plates in the COY anaerobic chamber; instead, the plates were placed in Kapak sealPAK pouches (Fisher Scientific) along with an Anaeropack sachet (Remel Inc., Chicago, IL) and then incubated at 37°C for 4 to 7 days. We found that using this method for

generating anaerobic conditions significantly increased recovery of *trans*-conjugates.

W83 whole-cell polyclonal antiserum and immunodiffusion analysis. Polyclonal antiserum was prepared as previously described with slight modifications (30, 52). In brief, New Zealand White rabbits were immunized intravenously with high concentrations (10 mg/ml in saline) of formalin-killed (0.5% for 1 h) whole bacterial cells of *P. gingivalis* strain W83. The rabbits were injected every other day with increasing amounts of the bacterial suspension (0.25, 0.5, 0.75, 1.0, 1.5, 2.0, and 2.5 ml). Final bleeds were performed 1 week after the final 2.5-ml injection. Antibody production was determined in an enzyme-linked immunosorbent assay using autoclaved formalin-fixed whole-cell suspensions. High antibody titers (~1:500,000) to K-antigen were detected. The immune serum was stored at −20°C until use. Double immunodiffusion analysis (Ochterlony assay) was performed with autoclaved bacterial cell suspensions, as previously described (30).

Microscopic examination. To examine for the presence of capsular polysaccharide, the cells were negatively stained with India ink (Fisher Scientific). The preparations were made by mixing a bacterial colony with 5 μl of India ink on a slide, which was then coverslipped and examined with a phase-contrast microscope at 1,000× magnification. In addition, for more-detailed analyses, cells were prepared for electron microscopy. Strains were grown on TSBHK agar plates for 24 h, pelleted, and then suspended in phosphate-buffered saline (PBS). The cells were then fixed at room temperature for 2 h with 3.6% glutaraldehyde in 0.1 M cacodylate buffer (pH 7.2) containing 0.075% ruthenium red and lysine (55 mM), followed by secondary fixation at room temperature in 2% osmium tetroxide in 0.1 M phosphate buffer (pH 7.2) for 1 h. The ruthenium red and lysine were added to the glutaraldehyde fixative in order to preserve polysaccharide-containing material. All samples were then dehydrated with a graded series of ethanol (10, 30, 50, 70, 90, and 100%) treatments of 15 min for each step. Samples were infiltrated with the acrylic resin LRWhite and polymerized for 24 h at 55°C. Ultrathin sections were cut with a diamond knife, and sections were picked up with copper grids (300 mesh) and viewed with a JEOL JEM-1200 EX transmission electron microscope.

SDS-PAGE analysis of crude polysaccharide preparations. To prepare crude polysaccharide samples, strains were grown to the mid-exponential growth phase in THBHK. Prior to extraction, the cells were washed once with PBS and then resuspended in buffer containing 0.05 M Na_2HPO_4 and 0.005 M EDTA. Cell-associated polysaccharides were extracted from cell pellets by the modified hot phenol-water extraction method (55). To compare amounts between mutant and parental strains, polysaccharides were extracted from 5 ml of culture (OD_{550}, 0.5). For profile analysis, 80-ml cultures were extracted. After extraction, the preparations were then dialyzed against distilled water and lyophilized.

For PAGE analysis, the lyophilized material was dissolved in PAGE sample buffer and heated at 100°C for 10 min. The entire lyophilized preparation from the 5-ml culture or aliquots (10 μl or 20 μl of a 5-μg/μl sample) from the 80-ml culture preparation were analyzed using 12% acrylamide gels. For alcian blue/silver staining, the gels were fixed in 100 ml of 40% ethanol, 5% acetic acid, and 0.005% alcian blue for 30 min. This was followed by a change to fresh alcian blue fixing solution (100 ml), and the gel was placed on a rocker overnight. After alcian blue fixation, the gel was rinsed in distilled water and oxidized in potassium dichromate for 10 min, following the manufacturer's protocol (Bio-Rad Laboratories). The gel was then rinsed with seven changes of deionized water (200 ml) and incubated for 20 min in silver reagent (Bio-Rad Laboratories). The gel was then quickly rinsed in water and incubated in developer until satisfactory staining was observed. Silver staining was stopped with the addition of acetic acid (5%).

Production of PG0121 recombinant protein. The ORF encoding the putative HU protein (PG0121) was amplified by PCR using the NdeI-tagged forward and XhoI-tagged reverse primers listed in Table 2. The amplicon was cloned into pGEMT-easy (Promega) and sequenced, and then the plasmid was digested with NdeI and XhoI. The insert was gel purified with QiaQuick purification kit (Qiagen) and subcloned in frame into the pET22b(+) vector (Novagen) for expression as a His-tagged fusion protein in *E. coli* BL21(DE3) (Novagen). To produce recombinant protein, a 500-ml LB culture was grown to an OD_{600} of ~1.0 and then induced with 1 mM isopropyl-β-D-thiogalactopyranoside or 5 h. The cell pellet (1 g) was lysed under denaturing conditions with 5 ml of lysis buffer (6 M guanidine hydrochloride, 10 mM sodium phosphate, 10 mM Tris-HCl; pH 8.0), and the His-tagged recombinant protein was purified from the supernatant by affinity chromatography on Ni^{2+}-nitrilotriacetic agarose (NTA; Qiagen). The preparation was concentrated with an Amicon Ultra concentration column with a molecular weight cutoff of 5,000 (Millipore). Protein concentrations were determined with the Bio-Rad protein assay kit using bovine gamma globulin as a standard.

Gel mobility shift assay. A target DNA probe of less than 500 bp is optimal for performing mobility shift assays. Since there are 513 bp between the inverted repeats, we chose to construct a probe in which this inner loop region was deleted. The DNA probe was generated by PCR using the F_106Lp and R_106Lp primer set listed in Table 2. This amplicon was cloned into pCRII-Topo (Invitrogen) and transformed into BL21(DE3) cells, and then the resulting plasmid was digested with NdeI and PpuMI, removing 503 bp from the internal loop region. The vector (pTstloop) was gel purified, treated with DNA terminator (Lucigen Corporation) to create blunt phosphorylated ends, and then religated and transformed into DH5α. This plasmid was then purified and used as a PCR template to generate the target probe (473 bp) by using the F_106Lp and R_106Lp primer set. In addition, we generated another probe (233 bp) containing the PG0106 promoter region (downstream of the DNA loop) by using primers F_106pr and R_106pr.

To perform the mobility shift assay, various amounts of PG0121 recombinant protein (rHU) were incubated with 100 ng of probe for 15 min at room temperature in 15 μl of binding buffer (final concentrations, 20 mM Tris-HCl [pH 8.0], 200 mM NaCl, 0.05 mg/ml bovine serum albumin, and 7% glycerol). Samples were loaded onto a 5% polyacrylamide gel (29:1) prerun for 1 h and then electrophoresed in 0.5× TBE (45 mM Tris, 45 mM boric acid, 1 mM EDTA). After electrophoresis, the DNA was stained with ethidium bromide for visualization.

The affinity of binding to the inverted repeat region using competition assays with digoxigenin (DIG)-labeled probes (DIG gel shift kit; Roche) was also evaluated. To perform this assay, 100 ng of recombinant PG0121 (rHU) was incubated with the DIG-labeled stem-loop probe (3 fmol) for 5 min in 15 μl of binding buffer (same as above) and then electrophoresed, as described above. The DNA was then transferred to a nylon membrane, and the DIG labeling was detected according to the manufacturer's instructions.

RESULTS

Genomic organization of the K-antigen capsule locus. The complete genome sequence of *P. gingivalis* strain W83 has been reported (40). The annotation in the CMR database (TIGR) predicted that the genes encoding PG0106 through PG0120 were part of an operon, and our previous studies confirmed this annotation (15). In addition, a previous report by Aduse-Opoku et al. (1) established that PG0106 through PG0120 encode the genes for the synthesis of K-antigen capsule. This capsule operon is flanked by two genes that are predicted to encode DNA binding proteins: PG0104, which is highly similar (57%) to DNA topoisomerase III from *Bacillus subtilis*, and PG0121, which has high similarity (72%) to the histone-like HU protein (β-subunit) from *Bacillus caldotenax*. As shown in Fig. 1A, these two genes are transcribed in the same direction as the capsule synthesis genes. Further analysis of the region led to the identification of a large (77-bp) inverted repeat located 5′ to PG0106 (Fig. 1A and B). One side of the inverted repeat begins 206 bp upstream of the PG0106 start codon, and its complement is located 477 bp downstream of the stop codon for PG0104. The loop consists of 513 bp. Secondary structure analysis and computations of this region using Mfold (57) showed that the inverted repeat region has a high potential to form a stem-loop structure with a predicted stability equivalent to a free energy of dissociation of -126 kcal mol^{-1}.

PG0104 and PG0121 are transcriptionally linked to the capsule operon. Genes PG0104 and PG0121 flank the capsule synthesis genes and are oriented on the chromosome in the same direction; therefore, we postulated that this locus encodes multiple transcripts, including one large polycistronic message encoding the entire region (PG0104 to PG0121). To evaluate this, we performed Northern blotting and RT-PCR analysis. For Northern analysis, three blots were prepared with RNA from wild-type (WT) W83 and DEL0106::Erm (capsule

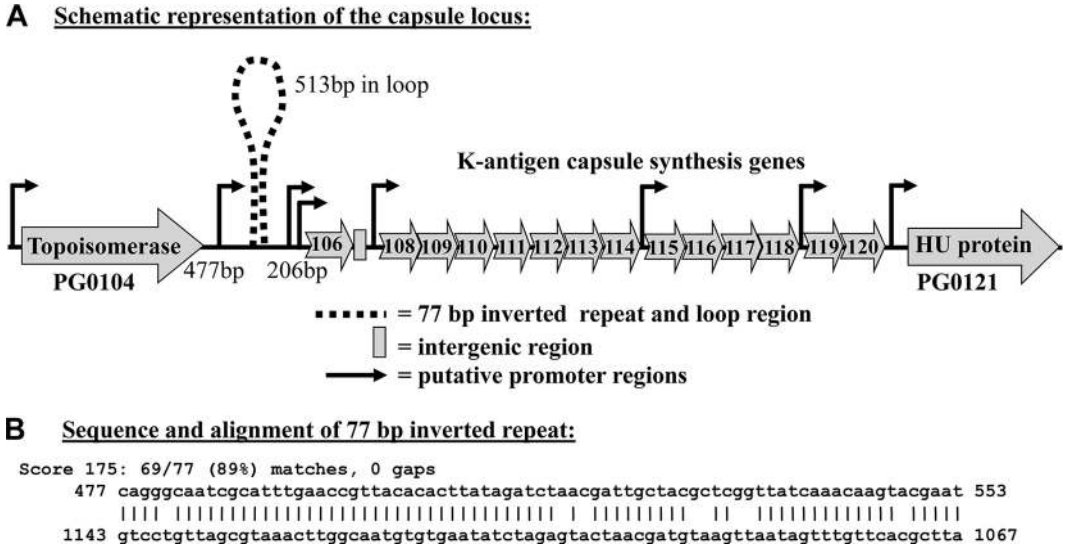

FIG. 1. Schematic representation of the capsule locus. (A) The position of the predicted hairpin structure created by base pairing of the 77-bp inverted repeat is indicated as a segmented line, and predicted promoter regions are shown with black arrows. The number of base pairs on either side of the hairpin and those contained within the loop are indicated. The ORF numbers correspond to TIGR CMR identifications. (B) Sequence and alignment of the 77-bp inverted repeat.

operon null mutant) cells in mid-exponential growth, as described in Materials and Methods. One blot was hybridized with a 233-bp probe for PG0106, which was previously shown to hybridize to the capsule operon transcripts (15). As shown in Fig. 2A, there was no hybridization in the DEL0106::Erm mutant (Δ106), and at least two transcripts (one greater than 9 kb and another region of ~5 kb) were detected in the parent strain W83 (WT). This result was consistent with our previously published results, showing that PG0106 is deleted and expression in the parent consists of at least two polycistronic transcripts. A second blot was hybridized with a 962-bp amplicon amplified from within the PG0104 ORF. As shown in Fig. 2B, two transcripts, one approximately 5 kb and another greater than 9 kb, were detected. Both of these transcripts are larger than the predicted 2-kb coding region for PG0104, indicating that the PG0104 ORF is encoded in at least two

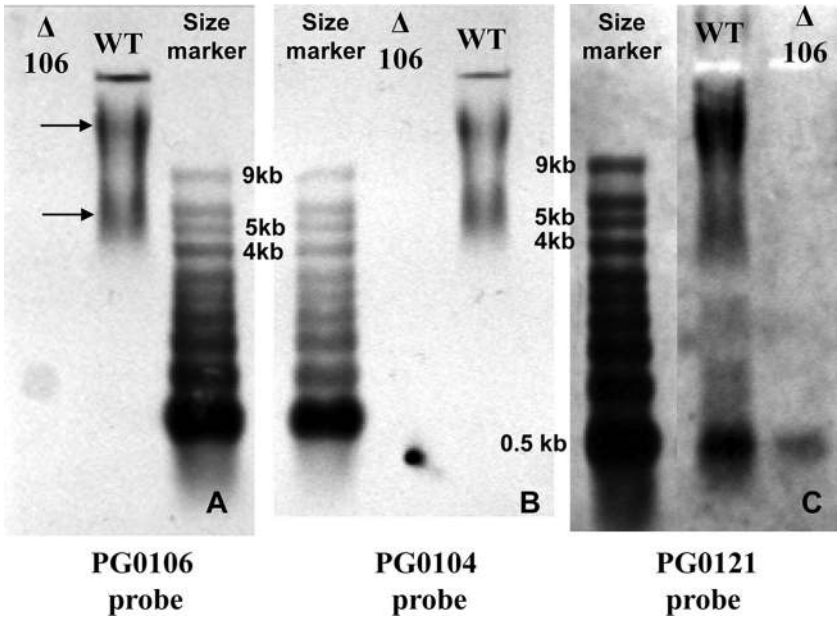

FIG. 2. Northern blot analysis of PG0106 (A), PG0104 (B), and PG0121 (C) expression in the PG0106 (capsule) mutant. Total RNA was isolated from WT strain W83 and DEL0106::Erm mutant (Δ106) cells in the mid-exponential growth phase, as described in Materials and Methods. Expression of the three genes (PG0104, PG0106, and PG0121) in the WT and the capsule operon null mutant (Δ106) are shown. The 10 size marker bands correspond to 9.0, 6.0, 5.0, 4.0, 3.0, 2.5, 2.0, 1.5, 1.0, and 0.5 kb. Arrows indicate hybridization to large transcripts (>9 kb) and transcripts in the 5- to 6-kb size range.

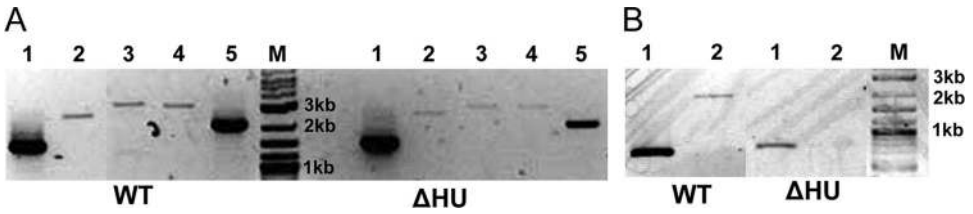

FIG. 3. RT-PCR analysis to evaluate transcriptional linkage of PG0121 to the capsule operon. Total RNA was isolated from the WT strain W83 and the DEL0121::Erm mutant (ΔHU), and cDNA was generated as described in Materials and Methods and using the MonsterScript cDNA synthesis kit. In the subsequent PCRs, the following primer combinations were used. (A) RT106_F/RT108_R (lane 1), RT108_F/RT110_R (lane 2), RT113_F/RT116_R (lane 3), RT116_F/RT118_R (lane 4), and RT118_F/RT120_R (lane 5); the gel shows linkage throughout the operon and the lower transcript levels of the K-antigen synthesis genes (except for PG0106 to PG0108) in the ΔHU mutant. (B) TIGR106_F/TIGR106_R (lane 1; positive control) and RT119_F/RT121_R (lane 2); the gel shows linkage of PG0121 to the capsule operon. M, DNA size markers.

polycistronic messages. Furthermore, these transcripts were not detected in the DEL0106::Erm mutant, indicating that PG0104 is transcriptionally linked to PG0106. The presence of a smaller (~5-kb) transcript when using PG0104 and PG0106 probes indicates that PG0104 and PG0106 along with the intergenic loop region are cotranscribed as a separate transcriptional unit, and this linkage was confirmed by RT-PCR (see below). In addition, although a 2-kb monocistronic message for PG0104 was not detected by Northern analysis, this does not rule out synthesis of this transcript, since the transcript may be unstable or the expression levels may be below the level of sensitivity obtained by nonradioactive Northern analysis.

The third blot was prepared and probed with a 137-bp amplicon amplified from within the PG0121 ORF (72% similarity to HU protein β-subunit). As shown in Fig. 2C, at least three transcripts, one greater than 9 kb, one approximately 4 kb, and another one around 300 bp in length, were detected in the wild-type strain. Two of these transcripts are larger than the predicted 300-bp coding region for PG0121, indicating that the PG0121 ORF is encoded in at least two polycistronic messages. These two larger transcripts were not detected in the DEL0106::Erm mutant, indicating that PG0121 is encoded in two separate capsule operon transcripts. The presence of the smaller transcript in the DEL0106::Erm mutant indicates that PG0121 is also transcribed separately.

Transcriptional linkage of PG0104 and PG0121 to the capsule synthesis genes (PG0106 to PG0120) was further evaluated using RT-PCR. As shown in Fig. 3, linkage throughout the operon and linkage of PG0121 to the K-antigen operon was confirmed. Furthermore, as shown in Fig. 4, transcription of the loop region, as well as linkage of PG0104 to the hairpin region and linkage of the hairpin to PG0106 were also confirmed, supporting the Northern analysis results showing that PG0104 and PG0106 are transcriptionally linked to the capsule synthesis locus.

Transcription of the capsule operon is downregulated in the absence of PG0121. To evaluate the effect of the loss of PG0121 on expression of the capsule operon, we performed Northern analysis. As shown in Fig. 5, two Northern blots were

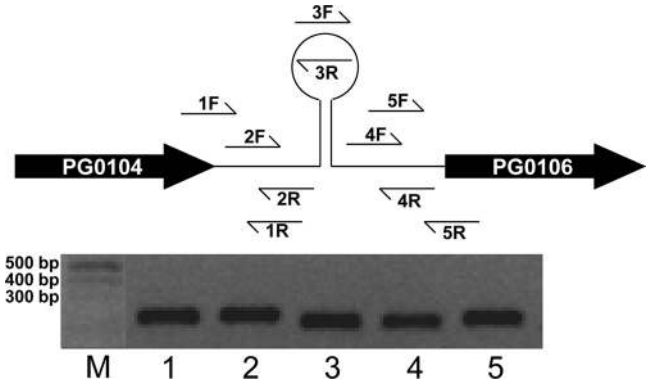

FIG. 4. RT-PCR analysis to evaluate transcriptional linkage of PG0104 to the 5′ end of the capsule operon and transcription through the hairpin region. Total RNA was isolated from the wild-type strain, and cDNA was generated as described in Materials and Methods with the QuantiTect reverse transcription kit. In the subsequent PCRs, the following primer combinations were used: RT_end104 (lane 1), RT_link104 (lane 2), RT_hairpin (lane 3), RT_link106 (lane 4), RT-_start106 (lane 5). The figure demonstrates linkage of PG0104 to the hairpin, transcription of the hairpin, and linkage of the hairpin to PG0106. M, DNA size markers.

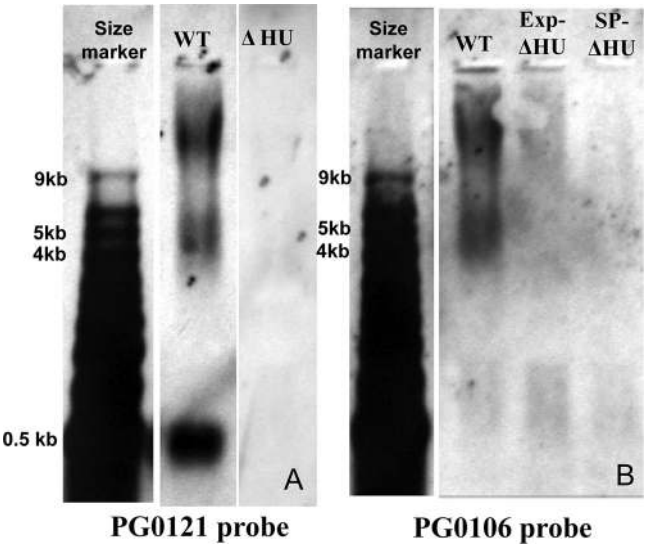

FIG. 5. Northern blot analysis of PG0121 (HU) and PG0106 (capsule operon) expression in the PG0121 (HU) mutant. Total RNA was isolated from WT strain W83 and the DEL0121::Erm mutant (ΔHU) as described in Materials and Methods. (A) Expression of PG0121 during exponential growth in strain W83 and the corresponding DEL0121::Erm mutant. (B) Expression of PG0106 during exponential growth in the parent strain W83 compared to expression during exponential (Exp) and stationary-phase growth (SP) in the corresponding DEL0121::Erm mutant, showing that the K-antigen capsule synthesis genes are downregulated in the ΔHU mutant.

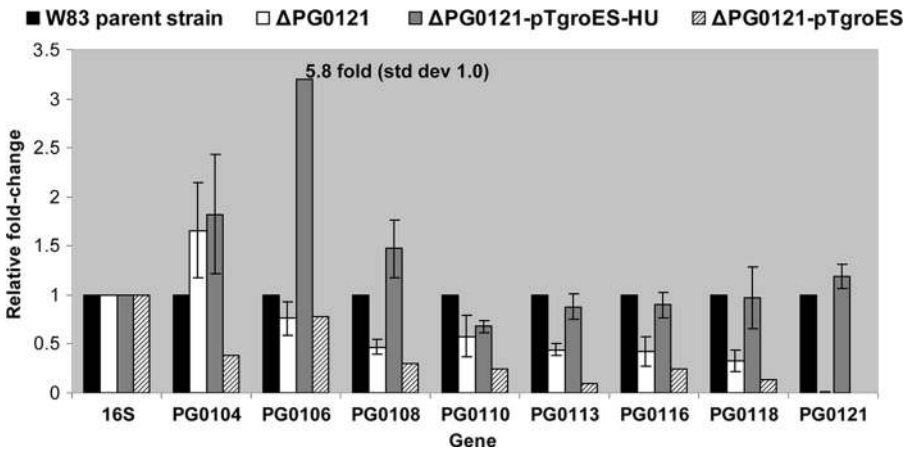

FIG. 6. qPCR analysis of K-antigen capsule synthesis genes in the PG0121 mutant and the complemented strain (pTgroES-HU). Total RNA was isolated from the parent strain W83, the DEL0121::Erm mutant (PG0121 mutant), and the complemented strain harboring plasmid pTgroES-HU, as described in Materials and Methods. To assess expression from all potential transcripts, cDNA was generated with random primers and the MonsterScript cDNA synthesis kit. The relative fold changes in expression shown are the averages of three separate experiments.

prepared. Blot A was prepared with RNA extracted from parent strain W83 and the corresponding PG0121 mutant during exponential growth; blot B was prepared with RNA from parent strain W83 during exponential growth and the corresponding HU mutant during both exponential and stationary phases of growth (OD_{550}, 1.2). One blot was hybridized with a 137-bp probe amplified from within the PG0121 ORF (blot A). As expected, at least three transcripts were detected in the wild-type strain when we used the PG0121 probe (one greater than 9 kb [largest size marker], one approximately 4 kb, and another one around 300 bp in length), and these transcripts were absent in the DEL0121::Erm mutant. Hybridization with the PG0106 (capsule operon) probe detected at least two large transcripts in the wild-type strain, as expected (blot B). However, these transcripts were not detected (or were found at very low levels) in the HU mutant during both the exponential and stationary phases of growth, indicating that PG0121 is required for stimulating transcription or stabilization of the capsule operon transcripts.

The expression levels of the genes in this locus in the parent strain and the DEL0121::Erm mutant were also compared using qPCR. For these analyses, the cDNA templates were generated using the MonsterScript cDNA synthesis kit, as described in Materials and Methods. The cDNA sample was generated with random primers (to assess expression from any transcript). As shown in Fig. 6, the overall expression of genes involved in K-antigen capsule synthesis were downregulated in the DEL0121::Erm mutant; however, although Northern analysis indicated that PG0104 expression was downregulated in the DEL0121::Erm mutant (large transcripts were not detected), qPCR analysis with random primers determined that expression of PG0104 was slightly upregulated in the DEL0121::Erm mutant.

Since Northern and RT-PCR analyses determined that PG0104 was transcriptionally linked to the capsule operon, the expression levels of this locus in the parent strain and the DEL0104::Erm mutant were compared using qPCR. For these analyses, the cDNA templates were again generated using the MonsterScript cDNA synthesis kit to ensure cDNA synthesis from large transcripts. No difference in expression of the capsule operon genes was detected in the PG0104 mutant (data not shown).

The HU mutant is deficient in surface polysaccharide expression. Immunodiffusion assays (Fig. 7C) determined that although transcription of the capsule operon was significantly downregulated in the PG0121 mutant, this strain still synthesizes K-antigen capsule. SDS-PAGE analysis of crude polysaccharide extracts was then used to evaluate the amount of polysaccharide produced. As shown in Fig. 7A, the mutant strain was deficient in the amount of capsule, similar to the K-antigen capsule null mutant ΔPG0106, while the amount of polysaccharide produced by the DEL0104::Erm mutant was the same as the parent strain W83. When the banding patterns of extracted polysaccharide were compared (Fig. 7B), the DEL0121::Erm mutant showed a similar profile to that of the parent strain, indicating that although the amount of polysaccharide is lower, the profiles are similar, unlike the DEL0106::Erm mutant, which was previously shown to be defective in both capsule (15) and LPS (38) synthesis.

To further investigate the effect of a PG0121 mutation on capsule production, we examined the W83 parent and the DEL0121::Erm mutant, as well as the DEL0106::Erm mutant (K-antigen minus strain) by electron microscopy, using a fixation method designed to preserve surface polysaccharides. As shown in Fig. 8, the DEL0106::Erm mutant lacked visible capsular material as expected, while the parent strain W83 exhibited a dense layer of capsular polysaccharide. The DEL0121::Erm mutant demonstrated an intermediate amount of capsular polysaccharide, less than the parent strain yet more than the nonencapsulated DEL0106::Erm mutant strain.

Complementation restored expression of capsular polysaccharide. As shown in Fig. 6, qPCR analysis determined that complementation of the DEL0121::Erm mutant with plasmid pTgroES-HU resulted in higher expression levels of all genes tested; however, complementation did not restore expression levels to those of the parent strain. In particular, the expression levels of PG0106 were significantly higher (5.8-fold) than that detected in the parental strain and the

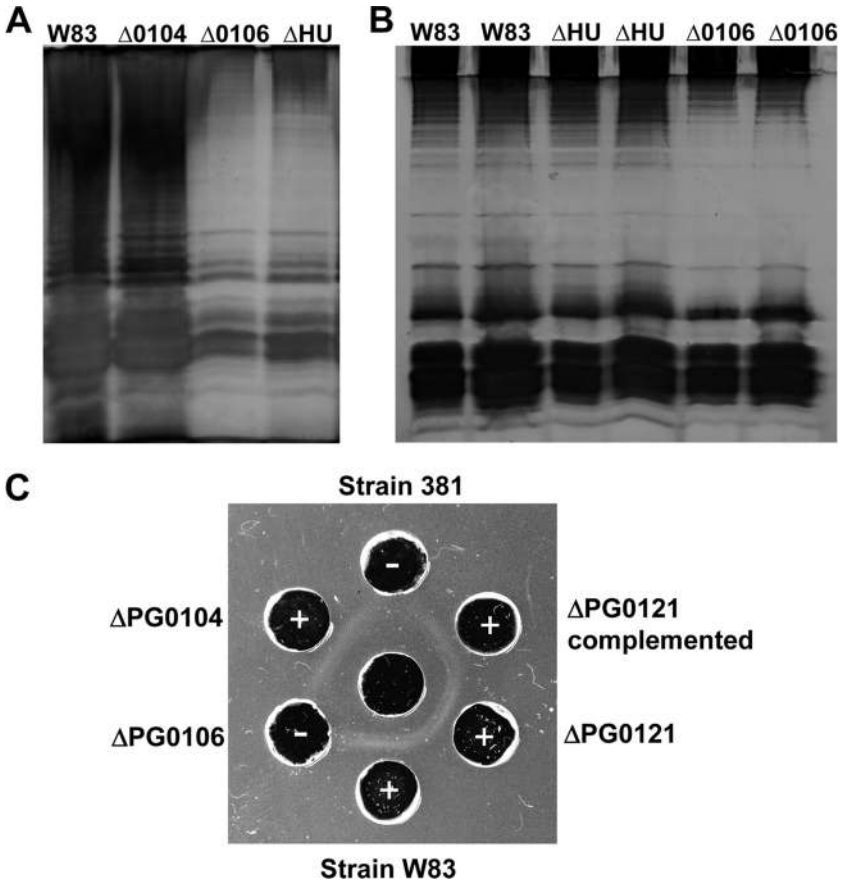

FIG. 7. Comparison of polysaccharide profiles of different strains based on PAGE. (A) Crude polysaccharide extracted from 5-ml cultures of the parent strain W83, the PG0104 mutant (Δ0104), the PG0106 mutant (Δ0106), and the PG0121 mutant (ΔHU) was analyzed by SDS-PAGE. Both the PG0106 and PG0121 mutants showed less capsule production than the parent W83 strain. The PG0104 mutant showed no change in capsule production and displayed a pattern similar to W83. (B) Polysaccharide profile analysis of the parent strain (W83), the PG0106 mutant (Δ0106), and the PG0121 mutant (ΔHU). For each strain, the left lane contained 50 μg of extracted polysaccharide and the right lane contained 100 μg. As expected, the PG0106 mutant exhibited less capsular polysaccharide and was lacking in a number of high-molecular-weight bands. However, the profile of the HU mutant was similar to the parent W83 strain, indicating that although the HUβ mutant is deficient in capsule production, the strain is not severely defective in biosynthesis of polysaccharides. (C) Double immunodiffusion assay results with antibodies to K-antigen capsule. All strains cross-reacted with the antiserum except for ΔPG0106 (the K-antigen null mutant) and strain 381, a K-antigen minus strain, indicating that neither a PG0104 nor a PG0121 mutation completely abolishes capsule production.

levels of PG0104 remained elevated, unaffected by complementation.

Northern blot analysis was also performed to determine if complementation with plasmid pTgroES-HU restored expression of the large transcripts. A blot was prepared with RNA isolated from the PG0121 mutant (ΔHU) and the PG0121 mutant harboring plasmid pTgroES-HU during exponential growth (Fig. 9). The blot was hybridized with a mixture of two probes: a 233-bp probe for PG0106 and a 137-bp PCR probe for the PG0121 ORF. As shown in Fig. 9, the large capsule operon transcript(s) was not detected in the PG0121 mutant (ΔHU). When the complementation plasmid pTgroES-HU was introduced, expression of the large transcript(s) was restored. Also, in the complemented strain, two smaller bands were detected, one (~500 bp) corresponding to PG0121 and another faint band around 1 kb, likely corresponding to the PG0106 monocistronic transcript. We believe that the diffuse nature of the signal results from overnight transfer of the RNA to the blot, which we found was required for effective transfer of large transcripts. We were able to obtain sharper banding patterns by running lower-percentage, larger gels and using electroblot transfer, demonstrating that as many as four transcripts greater than 9 kb encode PG0106 (see Fig. S1 in the supplemental material); however, this technique was not reproducible.

Transcription of another locus encoding genes involved in polysaccharide (APS) synthesis is downregulated in the absence of PG0121. Our microarray studies (data not shown) comparing the expression profile of the parent strain to the PG0121 mutant indicated that another locus involved in surface polysaccharide synthesis (PG1136 to PG1145) was also downregulated in the DEL0121::Erm mutant strain; therefore, we used qPCR analysis to support or refute these findings. As shown in Fig. 10, qPCR analysis confirmed these results. The expression levels of three genes in this locus (PG1137, PG1138, and PG1140) were examined and found to be downregulated. Thus, both the K-antigen synthesis genes (PG0106 to PG0120) and genes involved in

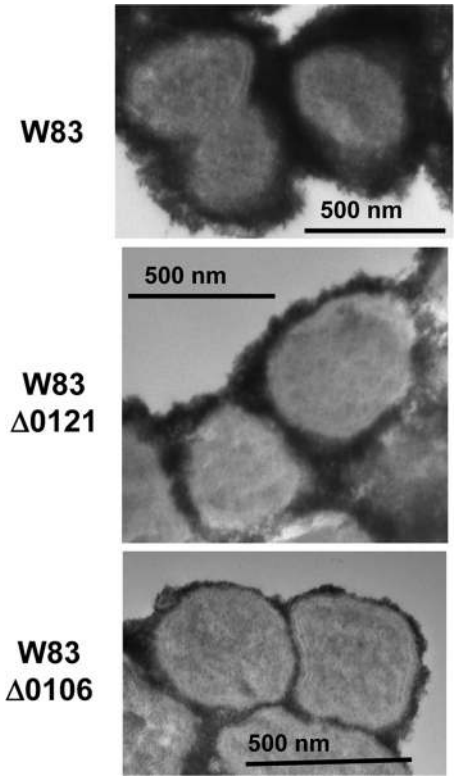

FIG. 8. Comparison of capsular structures by electron microscopy of the parent strain W83 with the K-antigen capsule minus mutant (Δ0106) and the ΔPG0121 (HU) mutant. Direct magnification levels of images were variable: W83 (×60,000); W83Δ0121 (×80,000), K-antigen capsule null strain W83Δ0106 (×100,000). The HU mutant strain produced less capsular polysaccharide than the parent strain W83.

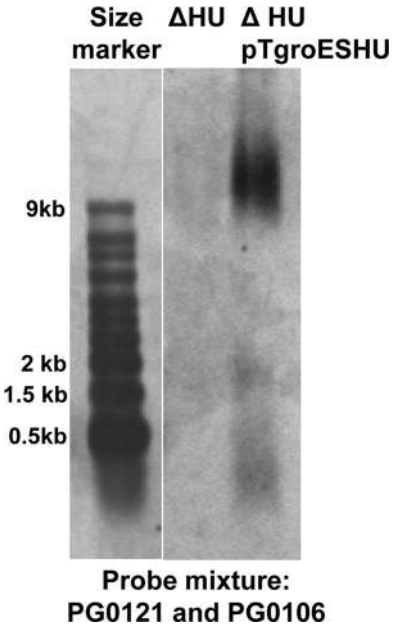

FIG. 9. Northern analysis of the complemented strain (pTgroES-HU) shows restoration of expression of large capsule operon transcripts. The blot was hybridized with a mixture of two probes: a 233-bp probe for PG0106 (capsule operon) and a 137-bp probe for PG0121 (HU). Shown is the expression of a large transcript(s) that was restored when HU was supplied in *trans* under the control of the *groES* (weak) promoter.

synthesis of another surface polysaccharide (APS) are downregulated in the DEL0121::Erm mutant.

A PG1258 (HUα) mutant could not be generated. Numerous attempts were made to create a PG1258 mutant; however, no DEL1258::Erm transformants could be obtained, providing preliminary data indicating that PG1258 encoding the HUα subunit is essential.

PG0121 recombinant protein binds DNA. In order to test the ability of the protein encoded by PG0121 (predicted to be HUβ) to bind *in vitro* to DNA, a His-tagged recombinant protein was overexpressed and purified. SDS-PAGE and Western analysis showed successful purification of this protein (rHU) (Fig. 11A and B). Mobility shift assays using this recombinant protein were performed as described in Materials and Methods. The target DNA probe consisted of the inverted repeats without the inner loop, resulting in a DNA probe of less than 500 bp (hairpin probe). As shown in Fig. 11C, the recombinant HU protein bound to the inverted repeat region upstream of PG0106, causing a shift in mobility on a polyacrylamide gel, even under stringent binding conditions (200 mM NaCl). However, only a partial shift in mobility was observed when a DNA probe consisting of only one side of the inverted repeat was used (Fig. 11D), indicating that the DNA binding protein encoded by PG0121 may have a strong affinity for the secondary structure, without sequence specificity. To further assess the affinity of recombinant PG0121 for the inverted repeat region, competition assays were performed (Fig. 11E). A supershift was observed with the addition of recombinant PG0121 (rHU; indicated with the arrow), and the addition of excess unlabeled probe (10 molar excess) competed for binding, indicating specificity for the probe. Taken together, although these studies are preliminary, our data indicate that PG0121 encodes a nonspecific DNA binding protein with high affinity for DNA with a secondary structure, which are known characteristics of HU proteins.

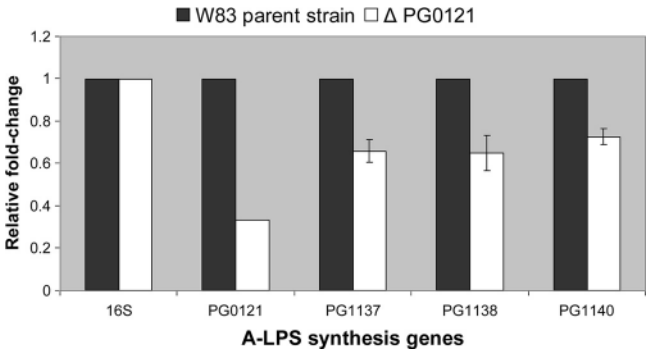

FIG. 10. qPCR analysis of the A-LPS synthesis locus (PG1136 to PG1145) in the PG0121 mutant. Total RNA was isolated in triplicate from the parent strain W83 and the DEL0121::Erm mutant (PG0121 mutant). To assess expression from all potential coding transcripts, cDNA was generated with random primers. The relative fold change of expression, showing downregulation of this locus in the HU mutant, is the average of three separate experiments.

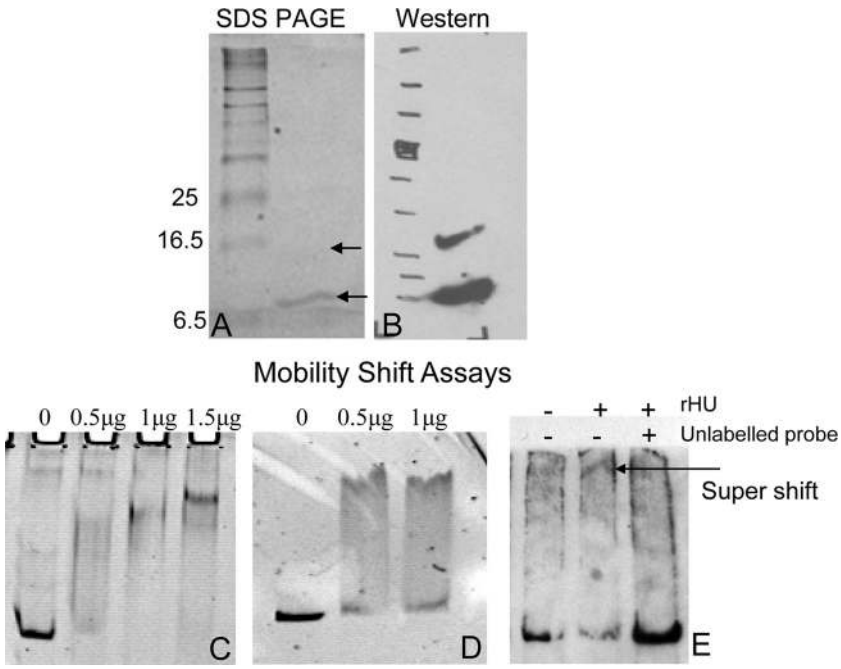

FIG. 11. Purification of recombinant PG0121 His-tagged fusion protein (HU) and gel mobility shift analysis of HU binding to the hairpin region. (A) SDS-PAGE analysis results, showing purification of the PG0121 His-tagged fusion protein. (B) Western blot results for the PG0121 His-tagged fusion protein, detected with anti-His tag antibodies. (C) Recombinant His-tagged PG0121 at the concentrations indicated was incubated with 100 ng of the inverted repeat target probe (see Materials and Methods for details) in a buffer containing high levels of salt (200 mM NaCl). (D) The same assay as shown in panel C was performed with a target probe of the promoter region minus the hairpin structure. (E) Competition assays using a DIG-labeled probe indicate high affinity for the hairpin (see Materials and Methods for details).

DISCUSSION

It was recently shown that IHF and H-NS, both histone-like global regulatory proteins, along with two other regulatory proteins (BipA and SlyA), control K5 capsule gene expression in *E. coli* (13, 48), hence providing precedence for histone-like proteins controlling expression of capsular polysaccharide. In this report, we present data indicating that the β-subunit of HU controls expression of the K-antigen capsule synthesis genes in the oral anaerobe *P. gingivalis*. Our data show that the gene PG0121, encoding HUβ, is cotranscribed with the large cluster of K-antigen capsule synthesis genes, and expression of these genes was downregulated in a PG0121 mutant. We also showed that transcription and production of the capsule can be restored through complementation with PG0121, thus providing clear evidence that expression of PG0121 affects expression of K-antigen capsule. As expected, we also identified HUβ as a nonspecific DNA binding protein. In addition, our data indicate that although HUβ does not interact specifically with the inverted repeat sequence, it does have a strong affinity for the secondary structure created by the 77-bp inverted repeat region, indicating that HU may directly control expression by interacting with this secondary structure. However, further studies are required to determine a direct role in regulation.

In *E. coli*, a change in the HUβ/HUα ratio, at the protein level, affects long-term survival (12) and cold adaptation (23), as well as capsule synthesis (43). Although it is evident that PG0121 expression affects transcript levels of the capsule operon, further studies at the protein level are required to develop a model as to how HUβ controls capsule expression. In addition, since our studies indicated that PG1258 (HUα) is essential, we are currently working to develop an inducible promoter system so we can best evaluate the potential role of both of the HU protein subunits. Our working hypothesis is that the two subunits work in concert to regulate gene expression and that the HUα subunit may be able to functionally compensate in the PG0121 mutant strain.

Another key finding from our studies was that PG0104, which is predicted to encode a DNA topoisomerase III (57% similarity), is also transcriptionally linked (at the 5′ end) to the K-antigen capsule synthesis genes. DNA topoisomerases are able to manipulate the topological state of DNA so that DNA transaction processes (replication, recombination, and transcription) can proceed without hindrance (54). During transcription, both positive and negative supercoils are generated on either side of the RNA polymerase. In essence, the need for topoisomerases during transcription is to sense supercoiling and either generate or dissipate it as they change the DNA topology (54). Most importantly, it has also been shown that DNA topoisomerase I works in concert with HU to maintain the required levels of supercoiling in *E. coli* (4, 41). In addition, it has been proposed that topoisomerases may play a role during the synthesis of very long transcripts, since there is the potential for the mRNA molecule to become entangled with the DNA template or with another transcript; however, there is no supporting evidence for this mechanism (54). Surprisingly, although our Northern blotting and RT-PCR data indicate PG0104 is transcriptionally linked to the capsule synthesis genes (PG0106 to PG0120) at the 5′ end, indicating that a

promoter upstream of PG0104 drives expression of a large capsule operon transcript, we discovered that expression of the capsule synthesis genes was not affected by a PG0104 mutation. Possible explanations for these finding are that although the topoisomerase encoded by PG0104 is transcriptionally linked to PG0106, other promoters downstream of the hairpin structure compensate and maintain expression of the capsule synthesis genes. Alternatively, another topoisomerase may compensate for a PG0104 mutation (there are at least five coding regions in the genome that show high similarity to topoisomerases). Further studies are required to determine a potential role for PG0104 in regulating expression of K-antigen capsule.

In this study, we also identified a large (77-bp) inverted repeat just upstream of the K-antigen capsule synthesis gene cluster that is predicted to form a hairpin structure with a predicted stability equivalent to a free energy of dissociation of -126 kcal mol^{-1}. The positioning of this element (5′ to the first gene in a cluster of genes involved in the same function) and the potential for this region to form a hairpin (cruciform structure) indicate that this element may be involved in regulating expression through antitermination. Antitermination is a regulatory mechanism that requires a regulatory protein to allow readthrough, thus preventing termination. In negatively supercoiled DNA (which can be generated by HU in the presence of topoisomerases), cruciform formation is actually favorable; therefore, regulation of transcription of the capsule operon by an antitermination mechanism is a strong possibility. In support of a role for antitermination, it was recently shown in *Bacteroides fragilis* (a close relative of *P. gingivalis*) that an important regulatory mechanism for expression of the large polysaccharide synthesis operons is antitermination (8). In addition, our qPCR data indicate upregulation of PG0104 expression in the HU mutant. Although these data are preliminary, increased levels of PG0104 transcription with decreased levels of the downstream genes would occur if the HU protein were required for readthrough. Some of our future studies are designed to determine if antitermination is involved in regulating expression of this transcript.

Another potential role for HU in controlling synthesis of K-antigen capsule is through RNA stability. Although cruciform formation of this element in DNA is not evident, the likelihood that this inverted repeat forms a stem-loop in the mRNA is very high; therefore, HU protein may bind this stem-loop, resulting in stabilization of the transcript. Hence, although we are only just beginning to explore the role of HU in controlling capsule expression and the function of the inverted repeat region, as well as its possible interaction with the topoisomerase encoded by PG0104, our working hypothesis is that functional interplay between HU and this conserved element is involved in controlling transcription and/or translation of this locus.

Cell surface polysaccharides often play a role in pathogenicity through several mechanisms, including immune evasion, immune modulation, attachment, and biofilm formation, as well as antiphagocytic activity. Neither K-antigen capsule nor A-LPS is an exception. In mice, strains that are encapsulated disseminate, causing a spreading type of infection, while K-antigen null strains typically result in localized abscesses and are significantly less virulent in soft tissue destruction (17, 31). Strains that are deficient in APS synthesis are more susceptible to killing by complement (50), indicating a role of A-LPS in the serum resistance of *P. gingivalis*. Our data indicate that transcription of the K-antigen capsule synthesis locus (PG0106 to PG0120) as well as genes in the APS (a phosphorylated branched mannan anchored to the surface by lipid A) synthesis locus (PG1136 to PG1145) are, in part, coordinated through the global regulatory protein HU. Specifically, microarray and quantitative PCR analyses using a PG0121 deletion mutant strain showed that PG0121 is involved in upregulating expression of both these loci. Our future studies are designed to determine if HU control of polysaccharide synthesis is a direct or indirect mechanism and to identify a potential HU regulon in *P. gingivalis*.

ACKNOWLEDGMENTS

This research was supported by grants R21DE17168 and R01DE1019117 (NIDCR) awarded to M.E.D.

We thank Heike Boisvert for her expertise in electron microscopy and Marty Taubman for guidance in generating antibodies.

REFERENCES

1. **Aduse-Opoku, J., J. M. Slaney, A. Hashim, A. Gallagher, R. P. Gallagher, M. Rangarajan, K. Boutaga, M. L. Laine, A. J. Van Winkelhoff, and M. A. Curtis.** 2006. Identification and characterization of the capsular polysaccharide (K-antigen) locus of *Porphyromonas gingivalis*. Infect. Immun. **74:**449–460.
2. **Balandina, A., L. Claret, R. Hengge-Aronis, and J. Rouviere-Yaniv.** 2001. The *Escherichia coli* histone-like protein HU regulates *rpoS* translation. Mol. Microbiol. **39:**1069–1079.
3. **Balandina, A., D. Kamashev, and J. Rouviere-Yaniv.** 2002. The bacterial histone-like protein HU specifically recognizes similar structures in all nucleic acids. DNA, RNA, and their hybrids. J. Biol. Chem. **277:**27622–27628.
4. **Bensaid, A., A. Almeida, K. Drlica, and J. Rouviere-Yaniv.** 1996. Cross-talk between topoisomerase I and HU in *Escherichia coli*. J. Mol. Biol. **256:**292–300.
5. **Bonnefoy, E., M. Takahashi, and J. R. Yaniv.** 1994. DNA-binding parameters of the HU protein of *Escherichia coli* to cruciform DNA. J. Mol. Biol. **242:**116–129.
6. **Boubrik, F., and J. Rouviere-Yaniv.** 1995. Increased sensitivity to gamma irradiation in bacteria lacking protein HU. Proc. Natl. Acad. Sci. U. S. A. **92:**3958–3962.
7. **Brunner, J., N. Scheres, N. B. El Idrissi, D. M. Deng, M. L. Laine, A. J. van Winkelhoff, and W. Crielaard.** 2010. The capsule of *Porphyromonas gingivalis* reduces the immune response of human gingival fibroblasts. BMC Microbiol. **10:**5.
8. **Chatzidaki-Livanis, M., M. J. Coyne, and L. E. Comstock.** 2009. A family of transcriptional antitermination factors necessary for synthesis of the capsular polysaccharides of *Bacteroides fragilis*. J. Bacteriol. **191:**7288–7295.
9. **Chen, T., K. Abbey, W. J. Deng, and M. C. Cheng.** 2005. The bioinformatics resource for oral pathogens. Nucleic Acids Res. **33:**W734–W740.
10. **Chen, T., H. Dong, Y. P. Tang, M. M. Dallas, M. H. Malamy, and M. J. Duncan.** 2000. Identification and cloning of genes from *Porphyromonas gingivalis* after mutagenesis with a modified Tn4400 transposon from *Bacteroides fragilis*. Infect. Immun. **68:**420–423.
11. **Choi, J. I., T. Nakagawa, S. Yamada, I. Takazoe, and K. Okuda.** 1990. Clinical, microbiological and immunological studies on recurrent periodontal disease. J. Clin. Periodontol. **17:**426–434.
12. **Claret, L., and J. Rouviere-Yaniv.** 1997. Variation in HU composition during growth of *Escherichia coli*: the heterodimer is required for long term survival. J. Mol. Biol. **273:**93–104.
13. **Corbett, D., H. J. Bennett, H. Askar, J. Green, and I. S. Roberts.** 2007. SlyA and H-NS regulate transcription of the *Escherichia coli* K5 capsule gene cluster, and expression of slyA in *Escherichia coli* is temperature dependent, positively autoregulated, and independent of H-NS. J. Biol. Chem. **282:**33326–33335.
14. **Cuthbertson, L., I. L. Mainprize, J. H. Naismith, and C. Whitfield.** 2009. Pivotal roles of the outer membrane polysaccharide export and polysaccharide copolymerase protein families in export of extracellular polysaccharides in gram-negative bacteria. Microbiol. Mol. Biol. Rev. **73:**155–177.
15. **Davey, M. E., and M. J. Duncan.** 2006. Enhanced biofilm formation and loss of capsule synthesis: deletion of a putative glycosyltransferase in *Porphyromonas gingivalis*. J. Bacteriol. **188:**5510–5523.
16. **Deghmane, A. E., D. Giorgini, M. Larribe, J. M. Alonso, and M. K. Taha.** 2002. Down-regulation of pili and capsule of *Neisseria meningitidis* upon

contact with epithelial cells is mediated by CrgA regulatory protein. Mol. Microbiol. **43:**1555–1564.
17. **Dierickx, K., M. Pauwels, M. L. Laine, J. Van Eldere, J. J. Cassiman, A. J. van Winkelhoff, D. van Steenberghe, and M. Quirynen.** 2003. Adhesion of *Porphyromonas gingivalis* serotypes to pocket epithelium. J. Periodontol. **74:**844–848.
18. **Dri, A. M., J. Rouviere-Yaniv, and P. L. Moreau.** 1991. Inhibition of cell division in *hupA hupB* mutant bacteria lacking HU protein. J. Bacteriol. **173:**2852–2863.
19. **Drlica, K., and J. Rouviere-Yaniv.** 1987. Histone like proteins of bacteria. Microbiol. Rev. **51:**301–319.
20. **Dzink, J. L., S. S. Socransky, and A. D. Haffajee.** 1988. The predominant cultivable microbiota of active and inactive lesions of destructive periodontal diseases. J. Clin. Periodontol. **15:**316–323.
21. **Fernandez, S., F. Rojo, and J. C. Alonso.** 1997. The *Bacillus subtilis* chromatin-associated protein Hbsu is involved in DNA repair and recombination. Mol. Microbiol. **23:**1169–1179.
22. **Fletcher, H. M., H. A. Schenkein, R. M. Morgan, K. A. Bailey, C. R. Berry, and F. L. Macrina.** 1995. Virulence of a *Porphyromonas gingivalis* W83 mutant defective in the prtH gene. Infect. Immun. **63:**1521–1528.
22a. **Gardner, R. G., J. B. Russell, D. B. Wilson, G. R. Wang, and N. B. Shoemaker.** 1996. Use of a modified *Bacteroides-Prevotella* shuttle vector to transfer a reconstructed β-1,4-D-endoglucanase gene into *Bacteroides uniformis* and *Prevotella ruminicola* $B_1$4. Appl. Environ. Microbiol. **62:**196–202.
23. **Giangrossi, M., A. M. Giuliodori, C. O. Gualerzi, and C. L. Pon.** 2002. Selective expression of the beta-subunit of nucleoid-associated protein HU during cold shock in *Escherichia coli*. Mol. Microbiol. **44:**205–216.
24. **Gonzalez, D., A. O. Tzianabos, C. A. Genco, and F. C. Gibson, 3rd.** 2003. Immunization with *Porphyromonas gingivalis* capsular polysaccharide prevents *P. gingivalis*-elicited oral bone loss in a murine model. Infect. Immun. **71:**2283–2287.
25. **Grossi, S. G., J. J. Zambon, A. W. Ho, G. Koch, R. G. Dunford, E. E. Machtei, O. M. Norderyd, and R. J. Genco.** 1994. Assessment of risk for periodontal disease. I. Risk indicators for attachment loss. J. Periodontol. **65:**260–267.
26. **Holt, S. C., L. Kesavalu, S. Walker, and C. A. Genco.** 2000. Virulence factors of *Porphyromonas gingivalis*. Periodontology **20:**168–238.
27. **Joseph, L. A., and A. C. Wright.** 2004. Expression of *Vibrio vulnificus* capsular polysaccharide inhibits biofilm formation. J. Bacteriol. **186:**889–893.
28. **Kjaergaard, K., M. A. Schembri, H. Hasman, and P. Klemm.** 2000. Antigen 43 from *Escherichia coli* induces inter- and intraspecies cell aggregation and changes in colony morphology of *Pseudomonas fluorescens*. J. Bacteriol. **182:**4789–4796.
29. **Kohler, P., and M. A. Marahiel.** 1998. Mutational analysis of the nucleoid-associated protein HBsu of *Bacillus subtilis*. Mol. Gen. Genet. **260:**487–491.
30. **Laine, M. L., B. J. Appelmelk, and A. J. van Winkelhoff.** 1997. Prevalence and distribution of six capsular serotypes of *Porphyromonas gingivalis* in periodontitis patients. J. Dent. Res. **76:**1840–1844.
31. **Laine, M. L., and A. J. van Winkelhoff.** 1998. Virulence of six capsular serotypes of *Porphyromonas gingivalis* in a mouse model. Oral Microbiol. Immunol. **13:**322–325.
32. **Lamont, R. J., and H. F. Jenkinson.** 1998. Life below the gum line: pathogenic mechanisms of *Porphyromonas gingivalis*. Microbiol. Mol. Biol. Rev. **62:**1244–1263.
33. **Lamont, R. J., and H. F. Jenkinson.** 2000. Subgingival colonization by *Porphyromonas gingivalis*. Oral Microbiol. Immunol. **15:**341–349.
34. **Li, S., and R. Waters.** 1998. *Escherichia coli* strains lacking protein HU are UV sensitive due to a role for HU in homologous recombination. J. Bacteriol. **180:**3750–3756.
35. **Miyabe, I., Q. M. Zhang, Y. Kano, and S. Yonei.** 2000. Histone-like protein HU is required for *recA* gene-dependent DNA repair and SOS induction pathways in UV-irradiated *Escherichia coli*. Int. J. Radiat. Biol. **76:**43–49.
36. **Moore, W. E., L. H. Moore, R. R. Ranney, R. M. Smibert, J. A. Burmeister, and H. A. Schenkein.** 1991. The microflora of periodontal sites showing active destructive progression. J. Clin. Periodontol. **18:**729–739.
37. **Morales, P., J. Rouviere-Yaniv, and M. Dreyfus.** 2002. The histone-like protein HU does not obstruct movement of T7 RNA polymerase in *Escherichia coli* cells but stimulates its activity. J. Bacteriol. **184:**1565–1570.
38. **Nakao, R., H. Senpuku, and H. Watanabe.** 2006. *Porphyromonas gingivalis galE* is involved in lipopolysaccharide O-antigen synthesis and biofilm formation. Infect. Immun. **74:**6145–6153.
39. **Nakayama, K., T. Kadowaki, K. Okamoto, and K. Yamamoto.** 1995. Construction and characterization of arginine-specific cysteine proteinase (arg-gingipain)-deficient mutants of *Porphyromonas gingivalis*. J. Biol. Chem. **270:**23619–23626.
40. **Nelson, K. E., R. D. Fleischmann, R. T. DeBoy, I. T. Paulsen, D. E. Fouts, J. A. Eisen, S. C. Daugherty, R. J. Dodson, A. S. Durkin, M. Gwinn, D. H. Haft, J. F. Kolonay, W. C. Nelson, T. Mason, L. Tallon, J. Gray, D. Granger, H. Tettelin, H. Dong, J. L. Galvin, M. J. Duncan, F. E. Dewhirst, and C. M. Fraser.** 2003. Complete genome sequence of the oral pathogenic bacterium *Porphyromonas gingivalis* strain W83. J. Bacteriol. **185:**5591–5601.
41. **Oberto, J., S. Nabti, V. Jooste, H. Mignot, and J. Rouviere-Yaniv.** 2009. The HU regulon is composed of genes responding to anaerobiosis, acid stress, high osmolarity and SOS induction. PLoS One **4:**e4367.
42. **O'Brien-Simpson, N. M., P. D. Veith, S. G. Dashper, and E. C. Reynolds.** 2003. *Porphyromonas gingivalis* gingipains: the molecular teeth of a microbial vampire. Curr. Protein Pept. Sci. **4:**409–426.
43. **Painbeni, E., M. Caroff, and J. Rouviere-Yaniv.** 1997. Alterations of the outer membrane composition in *Escherichia coli* lacking the histone-like protein HU. Proc. Natl. Acad. Sci. U. S. A. **94:**6712–6717.
44. **Pinson, V., M. Takahashi, and J. Rouviere-Yaniv.** 1999. Differential binding of the *Escherichia coli* HU, homodimeric forms and heterodimeric form to linear, gapped and cruciform DNA. J. Mol. Biol. **287:**485–497.
45. **Pontiggia, A., A. Negri, M. Beltrame, and M. E. Bianchi.** 1993. Protein HU binds specifically to kinked DNA. Mol. Microbiol. **7:**343–350.
46. **Rice, P., I. Longden, and A. Bleasby.** 2000. EMBOSS: the European Molecular Biology Open Software Suite. Trends Genet. **16:**276–277.
47. **Roberts, I. S.** 1996. The biochemistry and genetics of capsular polysaccharide production in bacteria. Annu. Rev. Microbiol. **50:**285–315.
48. **Rowe, S., N. Hodson, G. Griffiths, and I. S. Roberts.** 2000. Regulation of the *Escherichia coli* K5 capsule gene cluster: evidence for the roles of H-NS, BipA, and integration host factor in regulation of group 2 capsule gene clusters in pathogenic E. coli. J. Bacteriol. **182:**2741–2745.
49. **Schembri, M. A., D. Dalsgaard, and P. Klemm.** 2004. Capsule shields the function of short bacterial adhesins. J. Bacteriol. **186:**1249–1257.
50. **Slaney, J. M., A. Gallagher, J. Aduse-Opoku, K. Pell, and M. A. Curtis.** 2006. Mechanisms of resistance of *Porphyromonas gingivalis* to killing by serum complement. Infect. Immun. **74:**5352–5361.
51. **Swinger, K. K., and P. A. Rice.** 2004. IHF and HU: flexible architects of bent DNA. Curr. Opin. Struct. Biol. **14:**28–35.
52. **van Winkelhoff, A. J., B. J. Appelmelk, N. Kippuw, and J. de Graaff.** 1993. K-antigens in *Porphyromonas gingivalis* are associated with virulence. Oral Microbiol. Immunol. **8:**259–265.
53. **Wada, M., Y. Kano, T. Ogawa, T. Okazaki, and F. Imamoto.** 1988. Construction and characterization of the deletion mutant of *hupA* and *hupB* genes in *Escherichia coli*. J. Mol. Biol. **204:**581–591.
54. **Wang, J. C.** 2002. Cellular roles of DNA topoisomerases: a molecular perspective. Nat. Rev. Mol. Cell Biol. **3:**430–440.
55. **Westphal, O., and K. Jann.** 1965. Bacterial lipopolysaccharides extraction with phenol-water and further applications of the procedure, p. 83–92. *In* R. Whistler (ed.), Methods in carbohydrate chemistry, vol. 5. Academic Press, New York, NY.
56. **Whitfield, C.** 2006. Biosynthesis and assembly of capsular polysaccharides in *Escherichia coli*. Annu. Rev. Biochem. **75:**39–68.
57. **Zuker, M.** 2003. Mfold web server for nucleic acid folding and hybridization prediction. Nucleic Acids Res. **31:**3406–3415.